

Negative phase time for scattering at quantum wells: A microwave analogy experiment

R.-M. Vetter, A. Haibel, and G. Nimtz

Universität zu Köln, II. Physikalisches Institut, Zùlpicher Strasse 77, D-50937 Köln, Germany

(Received 27 June 2000; published 21 March 2001)

If a quantum mechanical particle is scattered by a potential well, the wave function of the particle can propagate with negative phase time. Because of the analogy of the Schrödinger and Helmholtz equations this phenomenon is expected to be observable for electromagnetic wave propagation. Experimental data for electromagnetic wells realized by waveguides filled with different dielectrics now confirm this conjecture.

DOI: 10.1103/PhysRevE.63.046701

PACS number(s): 41.20.-q, 03.65.-w

I. INTRODUCTION

The propagation of a wave packet is determined by the dispersion relation of the medium, e.g., in vacuum a plane wave propagates with a constant amplitude and a phase shift proportional to frequency. In the case of tunneling through a barrier, the almost constant phase leads to propagation speeds faster than the speed of light, calculated in [1] and measured for microwaves, single photons, and infrared light [2–4]. The exponential attenuation in the tunneling process limits the superluminal propagation to very short distances.

In the case presented here of particles scattered by a potential well instead of tunneling through a barrier, Li and Wang predicted a nonevanescent propagation, even with *negative* phase shifts [5]. Thus the transmitted signal is attenuated due only to reflections at the well's boundaries. A method for simulating the effects of multiple reflections inside the well using the impulse response function of the system is described in [6]. Negative phase shifts lead to propagation with negative group velocities, which means that it appears as if parts of a pulse are leaving the well before they enter. Recently this effect was demonstrated for stimulated emission, using the fact that the group velocity in the frequency regime between two closely spaced gain lines becomes $-c/310$, while the magnitude of the signal was amplified by 40% [7].

The potential well, in contrast, shows negative phase shifts in the frequency region between the highest bound state inside and the first resonance above the well. As in the case of a Fabry-Pérot interferometer, the limiting condition for signal transmission over large distances is that the frequency band where the effect occurs becomes narrower as the width of the well increases. However, in an interferometer the almost constant phase between two resonance frequencies leads to superluminal but still positive velocities

[8]. In the well, as a consequence of the frequency band limitation, only pulses of sufficient temporal width will show the effect of negative group velocity. The time span between cause and effect can be shortened, but, because of the finite pulse duration, cause and effect cannot be interchanged [9].

We present here an experimental simulation of the quantum well by a microwave setup using the analogy between the Schrödinger and Helmholtz equations. Applying the stationary phase approximation, the peak value of a quantum mechanical wave packet with a mean momentum $p_0 = \hbar k_0$ propagates with the group velocity $v_{gr} = (d\omega/dk)|_{k_0}$. This relationship can also be described in terms of classical mechanics by $v_{gr} = x/(d/d\omega)kx = x/\tau$, where particles traverse the distance x in the time τ . The term $kx = \varphi$ describes the change of phase for the considered distance, and $(d/d\omega)\varphi = \tau_\varphi$ is the time necessary for the propagation, called the *phase time* [1].

II. SCATTERING AT QUANTUM WELLS

In order to analyze a particle scattered by a potential well, the Schrödinger equation must be solved for a potential as sketched in Fig. 1 (left panel). However, the analogy between the Schrödinger and the Helmholtz equations (1) allows us to study the same process in an experiment with guided electromagnetic waves:

$$\left[\frac{d^2}{dx^2} + \frac{2m}{\hbar^2} [E - V(x)] \right] \psi(x) = 0,$$

$$\left[\frac{d^2}{dx^2} + \frac{1}{v^2} [\omega^2 - \omega_c^2(x)] \right] \phi(x) = 0. \quad (1)$$

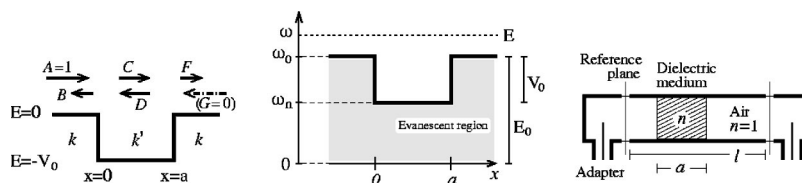


FIG. 1. Energy scheme of the quantum well, coefficients, and wave numbers of the wave function (left); microwave analogy using waveguide sections with different cutoff frequencies ω_0, ω_n (center); and the experimental setup (right): a waveguide of fixed length l is connected to a network analyzer by coaxial adapters. It partially contains a dielectric medium of refractive index n , which represents the quantum well.

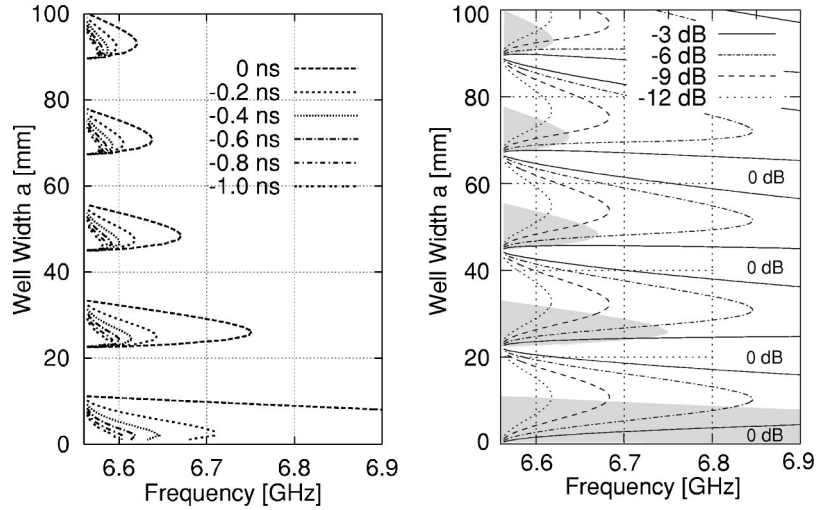


FIG. 2. Left: Regions of negative phase time τ_φ in a Teflon well according to Eq. (9). Depending on frequency f and well width a , negative phase times between 0 and -1 ns occur inside the marked regions. The abscissa starts at the cutoff frequency of the unfilled waveguide at 6.56 GHz; below this frequency only evanescent modes exist in the waveguide. Certain widths a yield negative phase times; the longer the well, the smaller the frequency band in which negative phase times appear. The region of negative phase time in the vicinity of $a=0$ reaches until approximately 7.6 GHz. Right: Transmission $|F|^2$ of the well calculated by Eq. (6). In the case of resonances the transmission reaches its maximum value 1 (0 dB). Regions of negative phase time (shaded) lie above each resonance. The attenuation inside these regions is independent of the well width.

In contrast to the case of quantum mechanics, here the phase and absolute value of the transmitted electromagnetic wave are measurable. Identical boundary conditions for the electromagnetic field ϕ (representing the E or H field) and the wave function ψ lead to an analogous solution of the propagation problem [10].

The energy level $V(x)$ of the quantum well can be constructed in a microwave experiment by waveguide sections with different cutoff frequencies $\omega_c(x)$ [see Fig. 1 (center)]. Applying the analogy, the energy baseline of the well is shifted by a constant value $E_0 = \hbar\omega_0$, which corresponds with the cutoff frequency ω_0 of the first waveguide section:

$$V(x) = \begin{cases} E_0, & x \leq 0 \\ E_0 - V_0, & 0 < x < a \\ E_0, & a \leq x. \end{cases} \quad \omega_c(x) = \begin{cases} \omega_0, & x \leq 0 \\ \omega_n, & 0 < x < a \\ \omega_0, & a \leq x. \end{cases} \quad (2)$$

We use the following ansatz for the wave function [see Fig. 1 (left)]:

$$\psi(x) = \begin{cases} Ae^{ikx} + Be^{-ikx}, & x \leq 0 \\ Ce^{ik'x} + De^{-ik'x}, & 0 < x < a \\ Fe^{ik(x-a)} + Ge^{-ik(x-a)}, & a \leq x. \end{cases} \quad (3)$$

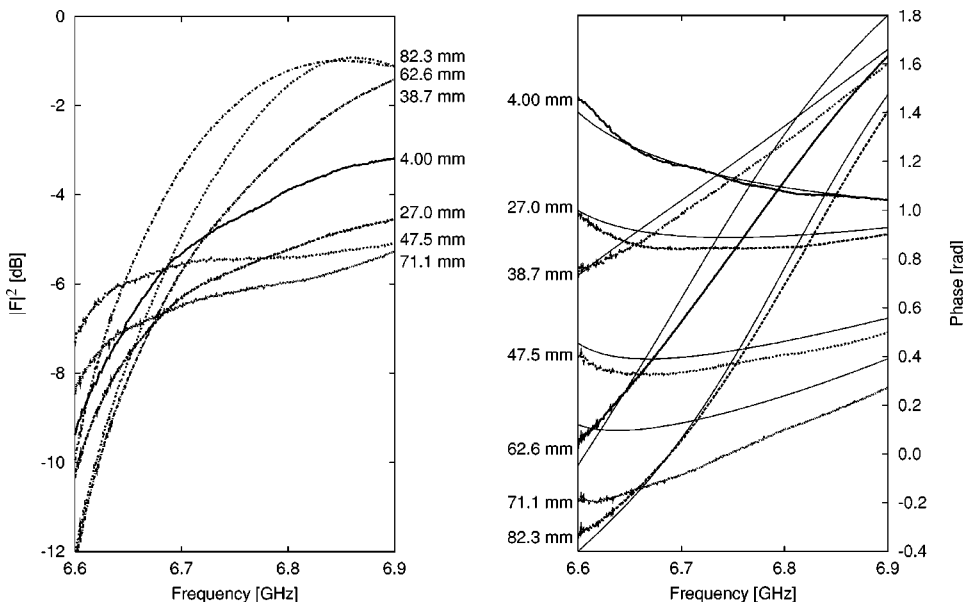


FIG. 3. Absolute value $|F|^2$ and phase φ of the transmission coefficient F vs frequency for different widths of Teflon pieces (i.e., wells). The absolute values are attenuated due to reflections at the discontinuities $x=0, a$ and by cutoff effects; peak values indicate resonances. For some widths ($a=4.0, 27.0, 47.5,$ and 71.1 mm) the phase φ drops with increasing frequency. Solid lines represent the theoretical phase progression (7). To achieve a clear representation, the phase curves are arranged in ascending order of the well widths.

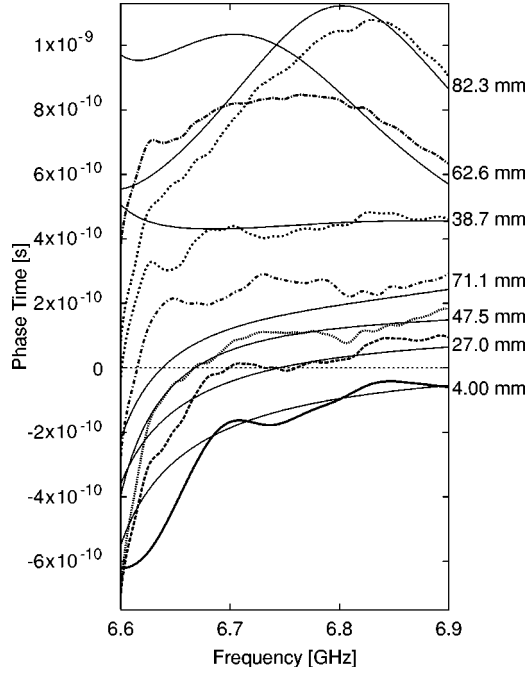


FIG. 4. Phase time τ_φ obtained from numerical derivation of the measured phase data of Fig. 3 and theoretical phase times (solid lines) calculated by Eq. (9). The curves for the well widths $a = 4.0, 27.0, 47.5,$ and 71.1 mm show negative phase times at frequencies near the cutoff frequency of the unfilled waveguide. The nonvanishing resistance of real waveguide walls, especially near the cutoff frequency, may cause the experimental deviations from the theoretical results.

This leads for energies $E > E_0$ to wave propagation with the real wave numbers

$$k = \frac{1}{\hbar} \sqrt{2m(E - E_0)} \quad \text{and} \quad k' = \frac{1}{\hbar} \sqrt{2m(E + V_0 - E_0)}. \quad (4)$$

Boundary conditions for the wave functions and their first derivatives at $x=0$ and a determine the unknown coefficients A, B, \dots, G of Eq. (3) (see [11]). Our definition of ψ for

$x \geq a$ implies that the complete phase shift inside the well occurs only in the coefficients F and G . Assuming an incident wave at $x=0$, we set $A=1$ and $G=0$ and find

$$F = \left[\cos k'a - \frac{i}{2} \left(\frac{k'}{k} + \frac{k}{k'} \right) \sin k'a \right]^{-1}. \quad (5)$$

Thus, the transmission of the well is given by

$$|F|^2 = \left[1 + \frac{1}{4} \left(\frac{k'}{k} - \frac{k}{k'} \right)^2 \sin^2 k'a \right]^{-1}, \quad (6)$$

and the complete phase shift of the transmitted wave at $x=a$ becomes

$$\varphi = \arg(F) = \arctan \left[\frac{1}{2} \left(\frac{k'}{k} + \frac{k}{k'} \right) \tan k'a \right]. \quad (7)$$

This formula is valid for both quantum mechanical and electromagnetic wells, while the phase time $\tau_\varphi = d\varphi/d\omega = (d\varphi/dk)(dk/d\omega)$ depends on the dispersion relation $k(\omega)$ of the well in question.

III. SCATTERING IN WAVEGUIDES

Inside the waveguide the wave numbers obey the dispersion relations

$$k(\omega) = \frac{1}{c} \sqrt{\omega^2 - \omega_0^2}, \quad k'(\omega) = \frac{n}{c} \sqrt{\omega^2 - \omega_n^2}, \quad (8)$$

where $c/n=v$ is the phase velocity in the medium. In the experimental setup a rectangular waveguide of length $l=250$ mm is used, which is partially filled by a dielectric medium of refractive index n [Fig. 1 (right)]. The cutoff frequencies of the empty and filled waveguide sections are $\omega_0 = \pi c/b$ and $\omega_n = \pi c/nb$, respectively, where b is the width of the waveguide. The X-band waveguide used ($b=22.86$ mm) has the cutoff frequency $f_0 = \omega_0/2\pi = 6.56$ GHz; filled with Teflon ($n=1.432$) the cutoff frequency becomes $f_n = \omega_n/2\pi = 4.58$ GHz. Thus, the energy

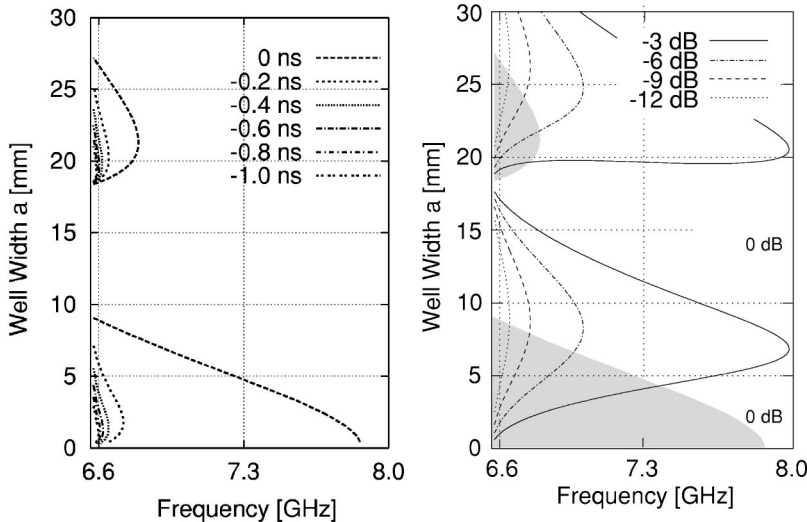


FIG. 5. Left: Regions of negative phase time τ_φ for wells made of Perspex, according to Eq. (9). The measurements were performed for the frequency interval between 6.6 and 8.0 GHz and for the well widths $a=6, 18,$ and 24 mm. The wells of width $a=6$ and 24 mm fulfill the conditions for negative phase time. Right: Transmission $|F|^2$ of the Perspex well.

levels of the quantum well correspond to $E_0 = \hbar \omega_0 = 27.1 \mu\text{eV}$ and $V_0 = \hbar(\omega_0 - \omega_n) = 8.2 \mu\text{eV}$. The phase time τ_φ , which describes the propagation of the maximum of a wave packet in the stationary phase approximation, is

$$\tau_\varphi = \frac{d\varphi}{d\omega} = \frac{a\omega}{c^2 k} \frac{2n^2 k^2 (k'^2 + k^2) - (k'^2 - k^2) k_0'^2 \sin(2k'a)/k'a}{4k^2 k'^2 + (k'^2 - k^2)^2 \sin^2 k'a} \quad (9)$$

with constant $k_0'^2 = k'^2 - n^2 k^2$. The high frequency limit [13] of Eq. (9) for $k, k' \rightarrow \infty$ is $\tau_\varphi = (a/c^2)(\omega/k)$. With the phase velocity $v_{\text{ph}} = \omega/k$ and the group velocity $v_{\text{gr}} = a/\tau_\varphi$, Eq. (9) results in the well known relationship $v_{\text{gr}} v_{\text{ph}} = c^2$ for waveguides.

In Fig. 2 (left panel) we plotted the regions of negative phase time depending on well width a and frequency f according to Eq. (9). The frequency range was chosen from the cutoff frequency of the empty waveguide 6.56 up to 6.9 GHz. The right diagram shows the transmission (6) of the well. Resonances occur for $k'a = \nu\pi$ where the transmission becomes 1, or, using Eq. (8), for the frequencies

$$f_\nu = \left[\left(\frac{c}{n} \frac{\nu}{2a} \right)^2 + f_n^2 \right]^{1/2} \quad (10)$$

with $\nu = 1, 2, \dots$ and $f_\nu > f_0$. By increasing the width of the well a the resonances are shifted to lower frequencies. A resonance shifted below the cutoff frequency f_0 turns into a bound state and the frequency regime close above this state shows a negative phase progression.

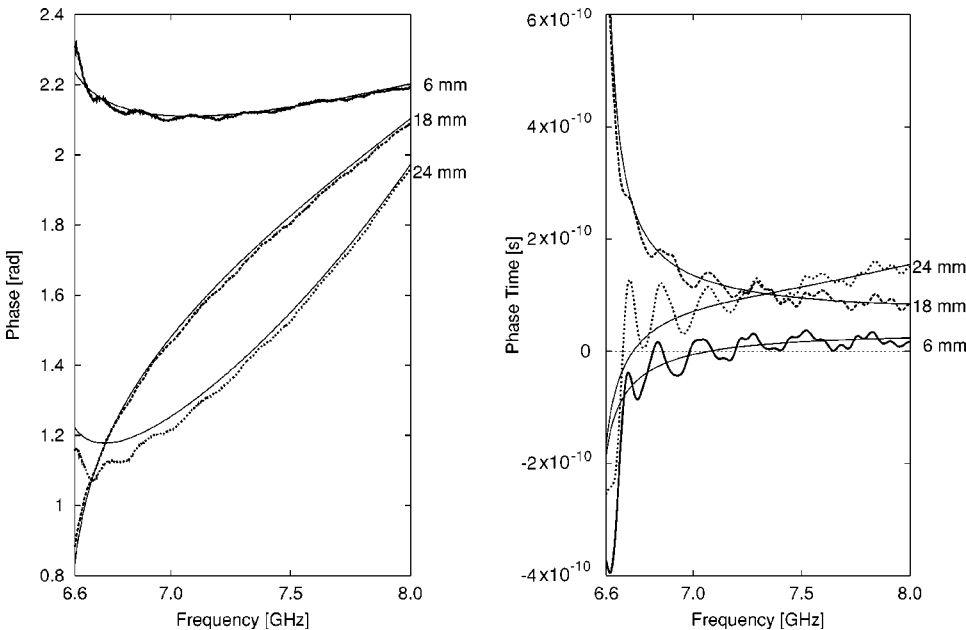


FIG. 6. Measured phase (left) and deduced phase time (right) for the Perspex wells. The phase progression is negative up to 7.1 GHz for the well of width $a = 6$ mm and up to 6.7 GHz for $a = 24$ mm. The oscillations around the theoretical curves (solid lines) are caused by an impedance mismatch between the waveguide and the connectors. The well width $a = 18$ mm lies outside the marked regions of Fig. 5; here, the phase shows a normal positive progression.

IV. MEASUREMENTS IN TEFLON WELLS

To verify the predictions we filled the waveguide with tight-fitting pieces of Teflon. Some of the pieces had widths that fulfilled the condition for negative phase time, lying inside the marked regions in Fig. 2, while other pieces should not show negative phase times because their widths lie in between.

For each piece of Teflon, the scattering parameter S_{21} for the transmission of the partially filled waveguide, which is defined as the ratio of the transmitted to the incident wave, was determined in the frequency domain. The measurements were performed with a network analyzer HP-8510, which allows an asymptotic measurement by eliminating undesired influences of the electrical connections by a calibration with two reference planes [Fig. 1 (right)] [12]. The measured transmission S_{21} has to be corrected by a factor describing the change of phase inside the unfilled waveguide sections of total length $l - a$:

$$F = S_{21} e^{-ik(l-a)}. \quad (11)$$

With this operation, the reference planes in Fig. 1 (right) are shifted to the surfaces of the Teflon block. We used the measured transmission function of the unfilled waveguide S_{21}^{ref} as a reference. Thus, the total phase shift inside the medium, which should comply with Eq. (7), is obtained from the measured data by

$$\varphi = \arg(S_{21}) - (l-a)\arg(S_{21}^{\text{ref}}). \quad (12)$$

Figure 3 shows $|F|^2$ and the phase φ of F for microwave transmission as a function of frequency across the well for different widths a . Maxima in the transmission $|F|^2$ indicate resonances; the theoretical values (10) for the wells of width $a = 62.6$ and 82.3 mm are $f_3 = 6.80$ and $f_4 = 6.85$ GHz, respectively. For $a = 38.7, 62.6,$ and 82.3 mm the phase in-

creases with increasing frequency, while for $a=4.0, 27.0, 47.5,$ and 71.1 mm the phase decreases near the cutoff frequency.

The phase time $\tau_\varphi = (2\pi)^{-1} d\varphi/df$ was calculated from the measured data by numerical derivation. Figure 4 presents the results for the phase time for transmission of the different Teflon pieces. For the well widths $a=4.0, 27.0, 47.5,$ and 71.1 mm, negative phase times appear, while the other wells show the normal behavior of a positive phase progression. The frequency intervals with negative phase times are in fair agreement with the predicted intervals in Fig. 2.

V. MEASUREMENTS IN PERSPEX WELLS

To add further credibility to the measured negative phase times we modified the well depth V_0 by using Perspex as an alternative dielectric medium with $n=1.6, f_n=4.10$ GHz, and $V_0=10.2 \mu\text{eV}$. According to Eq. (9), negative phase times are expected now for smaller well widths but for broader frequency bands (Fig. 5). Measurements were performed from 6.6 to 8.0 GHz and for well widths $a=6, 18,$ and 24 mm; the wells $a=6$ and 24 mm should show negative phase times. The measured phase progression in Fig. 6 (left) and the deduced phase times (right) are also in good agreement with the theoretical predictions for the Perspex wells

(thin lines). Although the well width $a=18$ mm lies close to a region of negative phase time, the measured phase progression of the well is clearly positive. This demonstrates how closely the appearance of negative phase time depends on the width of the potential well.

VI. CONCLUSIONS

The formal analogy between quantum mechanical and electromagnetic scattering has been investigated with microwaves. Theoretical studies [5] predicted negative phase times for certain well widths if the energy of an incident particle is less than half the well depth. In fact, our measurements at two different well depths show the predicted negative phase times. We have demonstrated the effect of negative phase time for potential scattering in a microwave analogy experiment.

ACKNOWLEDGMENTS

We are grateful to C.-F. Li and Q. Wang for providing their theoretical study prior to publication, and to P. Mittelstaedt for discussions on the theory of quantum mechanical scattering.

-
- [1] Th. Hartman, *J. Appl. Phys.* **33**, 3422 (1962).
 - [2] A. Enders and G. Nimtz, *J. Phys.* **I 2**, 1693 (1992).
 - [3] A. Steinberg, P. Kwiat, and R. Chiao, *Phys. Rev. Lett.* **71**, 708 (1993).
 - [4] Ch. Spielmann, R. Szipcs, A. Stingle, and F. Krausz, *Phys. Rev. Lett.* **73**, 2308 (1994).
 - [5] C.-F. Li and Q. Wang, *Phys. Lett. A* **275**, 287, (2000).
 - [6] Y. Japha and G. Kurizki, *Phys. Rev. A* **53**, 586 (1996).
 - [7] L. J. Wang, A. Kuzmich, and A. Dogariu, *Nature (London)* **406**, 277 (2000).
 - [8] J. Y. Lee, H.-W. Lee, and J. W. Hahn, *J. Opt. Soc. Am. B* **17**, 401 (2000).
 - [9] G. Nimtz, A. A. Stahlhofen, and A. Haibel, *Ann. Phys. (Leipzig)* (to be published), e-print physics/0009043.
 - [10] H. M. Brodowsky, W. Heitmann, and G. Nimtz, *Phys. Lett. A* **222**, 125 (1996).
 - [11] E. Merzbacher, *Quantum Mechanics*, 3rd ed. (Wiley, New York, 1998).
 - [12] H. J. Eul and B. Schiek, *IEEE Trans. Microwave Theory Tech.* **39**, 724 (1991).
 - [13] The high frequency limit of the refractive index $n(\omega)$ is 1, independent of the dielectric medium. So the term $(k'^2 - k^2)^2$ in the denominator of Eq. (9) becomes constant and can be neglected with respect to $4k^2k'^2$.